

This is the **accepted version** of the journal article:

Gómez-Orellana Seguí, Pablo; Lledós, Agustí; Ujaque Pérez, Gregori. «Computational analysis on the Pd-catalyzed C-N coupling of ammonia with aryl bromides using a chelate phosphine ligand». *Journal of organic chemistry*, Vol. 86, Issue 5 (March 2021), p. 4007-4017. DOI 10.1021/acs.joc.0c02865

This version is available at <https://ddd.uab.cat/record/274347>

under the terms of the  **CC BY** COPYRIGHT license

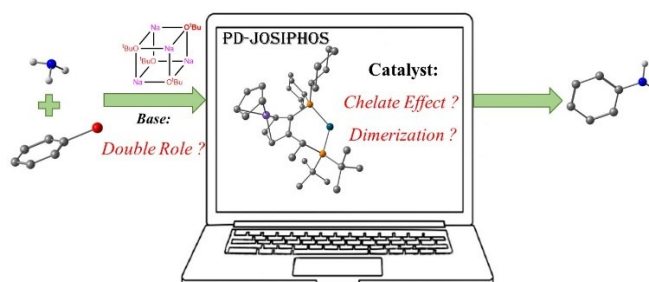
Computational Analysis on the Pd-Catalyzed C-N Coupling of Ammonia with Aryl Bromides Using a Chelate Phosphine Ligand

Pablo Gómez-Orellana, Agustí Lledós* and Gregori Ujaque*

Departament de Química and Centro de Innovació en Química Avanzada (ORFEO-CINQA), Universitat Autònoma de Barcelona, 08193 Cerdanyola del Vallès, Catalonia, Spain

email: agusti@klington.uab.es; email: gregori.ujaque@uab.cat

KEYWORDS DFT calculations, C-N Coupling, Pd catalyst, Reaction Mechanism, Ammonia



ABSTRACT The Buchwald-Hartwig amination of arylhalides with the Pd-Josiphos complex is a very useful process for the generation of primary amines using ammonia as reactant. DFT calculations are carried out to examine the reaction mechanism for this process. Despite the general mechanism for the C-N cross-coupling reaction is known, there are still some open questions regarding the effect of a chelate phosphine ligand and the role of the base on the process. Reaction pathways involving the release of one of the arms of the phosphine ligand are compared with those where the chelate phosphine remains fully coordinated. Conformational analysis for the complex with the open chelate phosphine is required to properly evaluate the proposed pathways. The role played by the added base ($t\text{-BuO}^-$) as a possible ligand or just as a base was also evaluated. The understanding of all these aspects allowed us to propose a complete reaction mechanism for the Pd-catalyzed C-N coupling of arylhalides with ammonia using the chelate Josiphos ligand.

INTRODUCTION

The Buchwald-Hartwig amination^{1,2,3,4,5} is a chemical reaction used in organic chemistry for the synthesis of carbon-nitrogen bond containing products. The reaction is a coupling of amines with aryl halides via a palladium-catalyst.^{6,7} This process has simplified the synthesis of pharmaceutical and agrochemical agents, among others relevant chemicals. It has advantages over other methods as good functional group compatibility and necessity of relatively mild conditions.^{8,9,10}

Primary and secondary amines are the common reactants in this type of coupling C-N reactions.¹¹ Nevertheless, the use of the ammonia, an inexpensive bulk chemical, is rather uncommon despite its potential for producing primary amines.¹² The major disadvantages of ammonia as reactant in homogenous catalysis are mainly related to its high basicity and strong N-H bond. The ammonia is a strong Lewis base that can cause the displacement of the

ligands of the metal complex generating stable intermediates that prevent the further development of the reaction.¹³ The application of homogenous transition metal catalyst for the selective synthesis of amines from ammonia under mild conditions is appealing, however, the development of such transformations is challenging; it would allow the functionalization of aryl and aliphatic chains to form primary amines.^{14,15,16}

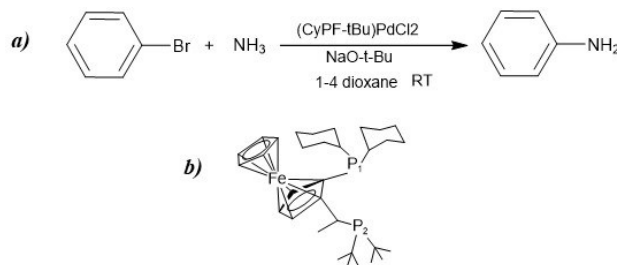


Figure 1: (a) C-N cross-coupling reaction using NH_3 developed by Hartwig's group. (b) Scheme of Josiphos (CyPF-tBu) ligand.

In 2006 Hartwig's group reported that a Pd complex along with the Josiphos chelate ligand was able to catalyse the coupling between ammonia and arylhalides (Figure 1).^{13,17,18} A related Pd-catalysed process for the coupling between aryls and ammonia was also developed by Buchwald using biaryl phosphines.^{19,20} These are among the few cases where ammonia was employed as reactant.^{21,22,23,24,25,26,27,28}

Understanding and rationalizing the synthetic tools that employ small reactants (i.e. NH_3 or H_2O) as starting material to produce higher added value chemicals is highly desirable.^{29,30,31,32,33} Computational chemistry is an excellent tool to investigate catalytic reactions.^{34,35} The reaction mechanism of the Buchwald-Hartwig amination considering the active Pd-catalyst with conventional phosphine ligands was initially described from a theoretical point of view by Cundari,³⁶ Harvey and Fey,³⁷ Organ³⁸ and Norrby³⁹ groups. More recently, the effect of biaryl phosphines, ylide-substituted phosphines and meta-terarylphosphine ligands were computationally evaluated by Baik,^{33,40} Ma,⁴¹ Gessner⁴², Jong and Lim⁴³ groups, respectively. The mechanism for Pd-NHC catalysed C-N coupling was also recently analysed.⁴⁴ The general mechanism is generally divided in four main steps (Figure 2):^{45,46,47,48,49,50,51} (i) oxidative addition of the aryl halide, (ii) amine coordination, (iii) amine deprotonation and halide release, and (iv) reductive elimination.

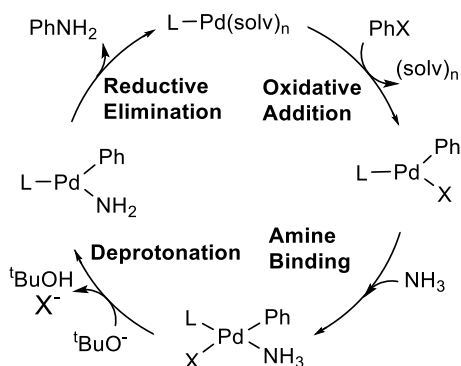


Figure 2: General catalytic cycle for Buchwald-Hartwig amination with monodentated phosphines (L).

The reaction mechanism for a bidentate ligand as Josiphos, however, has not been analysed in detail yet. Norrby made some useful suggestions in his mechanistic analysis, that was mostly focussed on the role of the base in the reaction, but without calculating the reaction profiles for the chelating system.³⁹ There are many particularities that are not known, as whether the chelate phosphine remains bicoordinated or not during the complete reaction, or if the *t*-BuO⁻ plays an exclusive role as a base or it also acts as a ligand during the substitution process. Thus, with the aim of providing an overall picture for the Buchwald-Hartwig

amination process for the NH_3 amine when a chelate biphosphine ligand as Josiphos is employed, we performed a computational analysis of the reaction mechanism.

RESULTS AND DISCUSSION

The general reaction mechanism for the Buchwald Hartwig amination can be divided in four main steps as shown in Figure 2.^{37,39} The oxidative addition and reductive elimination steps should not be significantly affected by a chelate phosphine. The amine binding, however, could be significantly modified. Moreover, in addition to the amine, the base may also coordinate the catalyst; thus, deprotonation can be also modified. Therefore, for analytical purposes the possibility for ligand substitution and proton transfer are considered together.

The first and third sections describe the results for the oxidative addition and reductive elimination steps. The second one is divided in four subsections each one devoted to each of the alternatives for the ligand substitution process / deprotonation that has been considered. Finally, the last section collects all the results and describes the overall mechanistic proposal.

Oxidative Addition

The catalytic cycle starts with the interaction of the aryl bromine with Pd-Josiphos complex, **I**. The Pd-Josiphos is an asymmetric phosphine, thus, the oxidative addition of PhBr may take place through two different pathways depending on the relative position of halide and phenyl within the square planar intermediate. The formation of a complex with the phenyl *trans* to P₂, intermediate **II**, located at -18.3 kcal mol⁻¹, must overcome an energy barrier of 8.7 kcal mol⁻¹, **TS_I** (Figure 3). The product of the oxidative addition for the pathway giving rise to the phenyl group *trans* to P₁, intermediate **II_{op}**, has a Gibbs energy of -14.5 kcal mol⁻¹; the transition state, **TS_I_{op}**, has an energy of 13.4 kcal mol⁻¹ (Figure 3).

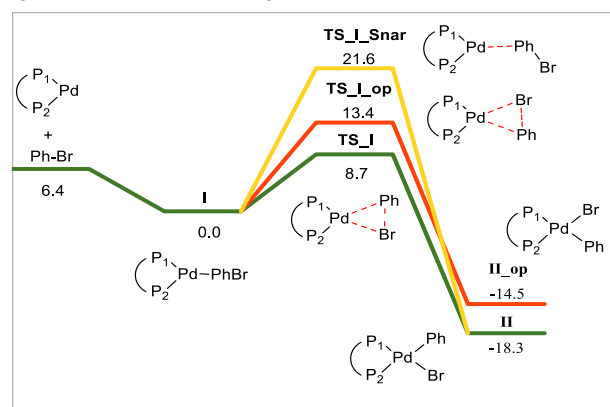


Figure 3: Gibbs energy profiles for the oxidative addition in 1-4 dioxane (kcal mol⁻¹).

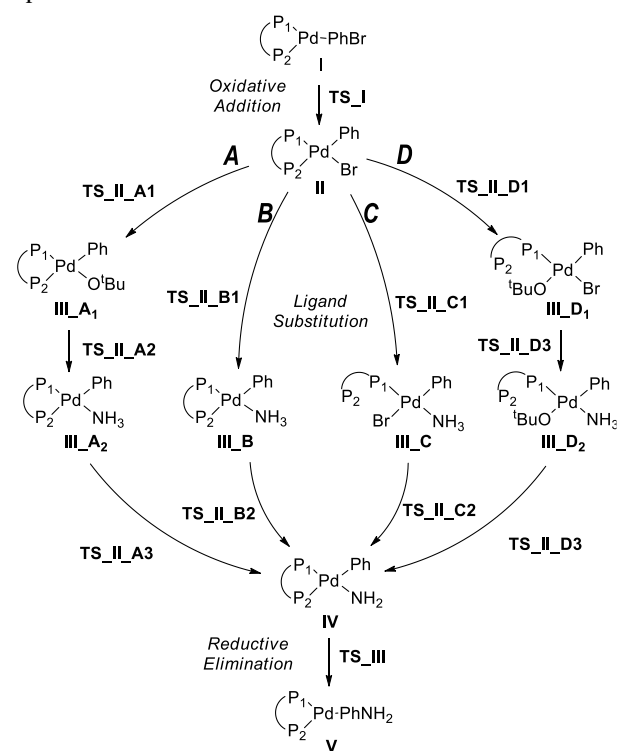
The oxidative addition through an aromatic nucleophilic substitution path (*S_NAr*) was also evaluated.^{52,53,54,55} The

transition state **TS_I_Snar** is located at 21.6 kcal mol⁻¹ compared to intermediate **I**. The Gibbs energy barrier is 12.9 kcal mol⁻¹ higher than that for **TS_I**, therefore, it can be discarded for this process in agreement with other works.^{52,56,57}

The most accessible pathway for the addition gives rise to intermediate **II**, with the phenyl group *trans* to P₂ and the bromide *trans* to P₁. Both, the relative energy barrier (by 4.7 kcal mol⁻¹) and stability (by 3.8 kcal mol⁻¹) support the formation of intermediate **II** over intermediate **II_{op}**. This step is irreversible (*vide infra*), thus, the subsequent steps of the reaction mechanism are analysed from this intermediate.

Ligand Substitution and proton transfer

For the steps involving ligand substitution and proton transfer processes we envisioned four different pathways as represented in Scheme 1. The difference between the two first pathways, both keeping the phosphine chelate coordinated along the reaction, is related to the role played by the base in the mechanism. In pathway A the t-BuO⁻ substitutes the halide in the coordination sphere of the metal, and then it is replaced by the ammonia; the t-BuO⁻ plays a double role, as a ligand and as a base. In pathway B, the halide is substituted directly by NH₃, and the t-BuONa acts exclusively as a base subtracting the proton. Pathways C and D are analogous but taking into consideration that the phosphine can dissociate one of the arms thus offering an open coordination site.



Scheme 1: Reaction pathways evaluated for the Buchwald-Hartwig amination with ammonia catalysed by Pd-Josiphos.

Pathway A

In this pathway the t-BuO⁻ plays a double role as a nucleophile substituting the bromide in the coordination sphere of palladium, and as a base deprotonating the coordinated ammonia.

The Gibbs energy reaction profile is shown in Figure 4. Intermediate **II_A**, with a relative energy of -14.2 kcal mol⁻¹ due to the presence of the (t-BuONa)₄ cluster, undertakes two consecutive ligand replacements on the complex. In the first one, a t-BuO⁻ substitutes the Br⁻ in the coordination sphere of the metallic center; the transition state **TS_II_A1** is located at 10.2 kcal mol⁻¹, with a relative Gibbs energy barrier of 28.5 kcal mol⁻¹. This step involves not only a ligand replacement but also the dissociation of one of the t-BuO⁻ anions from the cluster. The transition state shows a trigonal bipyramidal geometry around the Pd center, with Ph and P₂ occupying the apical positions, respectively (Figure 5). The intermediate formed, **III_{A1}**, where t-BuO⁻ has replaced Br⁻ has a Gibbs energy of -10.0 kcal mol⁻¹, (Figure 5). Then there is the substitution of the base (t-BuO⁻) by the amine (NH₃) along with the proton transfer from NH₃ to the t-BuO⁻. The relative Gibbs energy barrier for this step, **TS_II_A2**, is 13.5 kcal mol⁻¹. It involves a ligand replacement along with amine deprotonation giving rise to intermediate **IV_{base_A}**, located at -15.2 kcal mol⁻¹. This intermediate is ready for the reductive elimination process (see below).

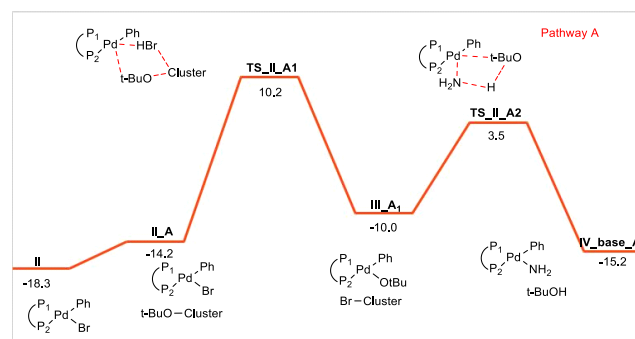
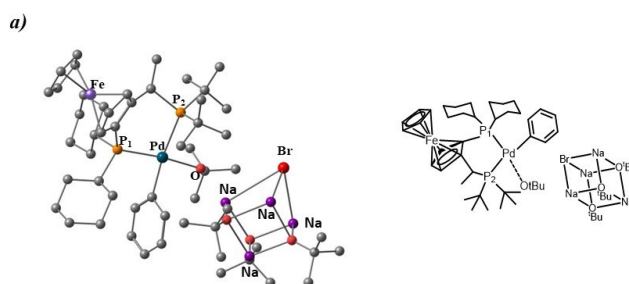


Figure 4: Gibbs Energy profile for pathway A. Gibbs energies in kcal mol⁻¹.



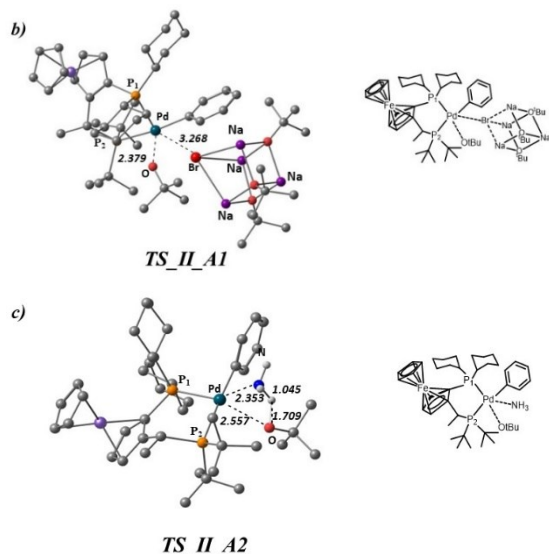


Figure 5: Optimized geometries for: (a) **III_{A1}**, (b) **TS_{II_A1}**, and (c) **TS_{II_A2}**. Distances in Å.

- Pathway B

This pathway considers that t-BuO⁻ only plays a role as a base in the reaction. The Gibbs energy profile is shown in Figure 6. The replacement of the bromine by ammonia takes place through **TS_{II_B}**; it presents a trigonal bipyramidal geometry with the incoming NH₃ and leaving Br⁻ at equatorial positions (Figure 7). The relative Gibbs energy barrier is 20.8 kcal mol⁻¹. The intermediate formed, **III_{B1}**, has a relative Gibbs energy of -16.6 kcal mol⁻¹. The calculation of the proton transfer from coordinated NH₃ to the base considers the latter in its cluster form. Thus, intermediate **III_{B2}**, including the cluster is at -6.1 kcal mol⁻¹. The energy barrier for the proton transfer, **TS_{III_PT}**, was estimated to be 12.7 kcal mol⁻¹ from **III_{B1}**.⁵⁸ The intermediate formed, **IV_{Base}**, with a relative Gibbs energy of -10.0 kcal mol⁻¹, is analogous to that of the previous pathway and ready for the reductive elimination.

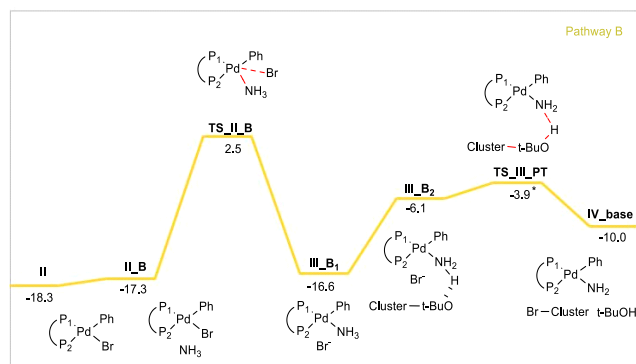


Figure 6: Gibbs energy profile for Pathway B in 1-4 dioxane (kcal mol⁻¹). * Value estimated in the absence of Br⁻ from the calculation.

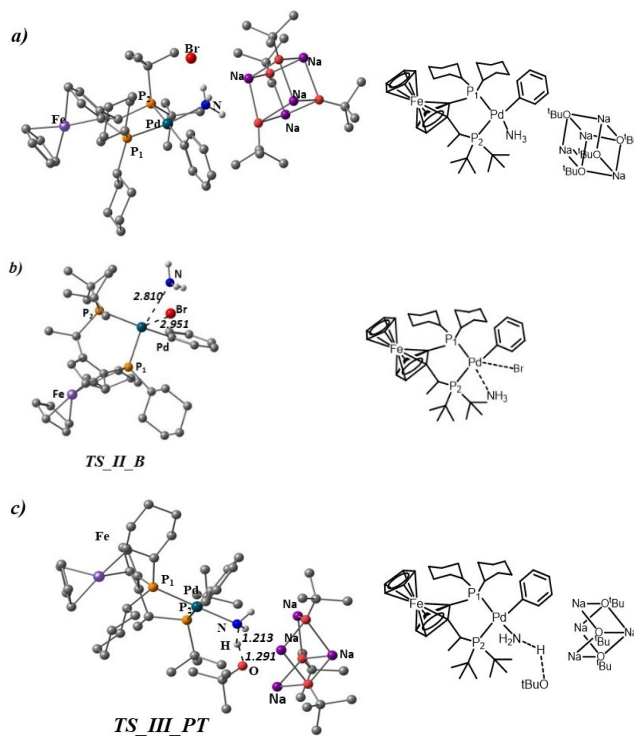


Figure 7: Optimized geometries for: (a) **III_{B2}**, (b) **TS_{II_B}** and (c) **TS_{III_PT}**. Distances in Å.

For both pathways A and B, five coordinated intermediates for the ligand substitution were searched. Nevertheless, as expected for a Pd(II) complex, they could not be located on the potential energy surface. Only transition states for the ligand substitution showed trigonal bipyramidal geometries (Figures 5 and 7).

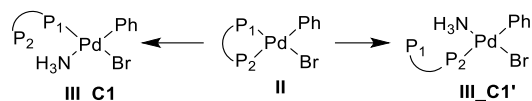
Pathways A and B consider the chelating phosphine fully coordinated along the path. Pathway B is preferred over A since the ligand substitution of Br⁻ by NH₃ is favoured over its substitution by t-BuO⁻. In pathway A, the proton transfer is a barrierless process once NH₃ is coordinated to the Pd center, because the t-BuO⁻ has been previously dissociated through transition state **TS_{II_A1}**. In pathway B, however, it is necessary to overcome a low energy barrier of 2.2 kcal mol⁻¹ (from **III_{B2}** to **TS_{III_PT}**; Figure 6) due to the dissociation of the t-BuO⁻ from the cluster.

- Pathway C

The next two pathways describe parallel mechanisms to those previously described but considering that one of the arms of the chelate phosphine can dissociate. The dissociation of the phosphine generates an additional issue regarding the conformational flexibility since there are many conformational possibilities for the monodentate Josiphos phosphine. To overcome this issue, we performed a conformational analysis for such an intermediate.

In pathway C the first step is the replacement of a phosphine arm by the ammonia ligand. For an asymmetric phosphine such a replacement can generate two different

intermediates depending on the substituted phosphine (Scheme 2).



Scheme 2: Dissociation of the phosphine arms by the nucleophilic attack of the ammonia: P₂ (**III_C1**) and P₁ (**III_C1'**).

For the conformational analysis we first developed the force field parameters for the metal center (see computational details). Then MD calculations were run at high temperature (1000 K) to explore the conformational space. Finally, the structures saved during MD were clustered to obtain the most representative conformations for each intermediate. These structures were subsequently optimized at QM level to check their relative Gibbs energies (see Supporting Information). A similar conformational study was performed for each of the two possible intermediates, **III_C1** and **III_C1'** (Scheme 2). The results are gathered in Table 1. The values obtained point out the importance of conformational effects when computing catalytic cycles with flexible ligands.^{35,59,60}

Conformations related to **III_C1'** intermediate are in the range of 8 to 30 kcal mol⁻¹, always much higher in energy. Thus, they will not be further considered. For **III_C1** intermediate, the most stable one (conf. 4) was selected to study this reaction pathway. There are other conformations that may be also suitable for this mechanism, but for analytic purposes we selected this one (it does not modify the conclusion of the work because this is the most favoured pathway).

Table 1: Gibbs relative energies (kcal mol⁻¹) for conformers of intermediates **III_C1**, **III_C1'** and **III_C2**.

Conformations	$\Delta\Delta G_{\text{solv}}$	$\Delta\Delta G_{\text{solv}}$	$\Delta\Delta G_{\text{solv}}$
	III_C1	III_C1'	III_C2
Conf. 1	4.8	10.7	2.7
Conf. 2	6.2	16.4	-2.2
Conf. 3	3.7	11.3	0.5
Conf. 4	0.0 ^a	10.6	2.3
Conf. 5	0.7	8.1	4.5
Conf. 6	2.8	21.1	16.8
Conf. 7	5.1	21.7	11.2
Conf. 8	10.6	29.8	11.4
Conf. 9	17.1	10.3	2.5
Conf. 10	10.9	27.4	4.3

^a This conformation has a relative Gibbs energy of -9.8 kcal mol⁻¹ within reaction profile in Figure 8.

The Gibbs energy profile for pathway C is represented in Figure 8. The transition state for the first step, **TS_II_C1** (Figure 9), is located at -1.2 kcal mol⁻¹, with a relative Gibbs energy barrier of 17.1 kcal mol⁻¹. The intermediate formed, **III_C1** has a relative Gibbs energy of -9.8 kcal mol⁻¹. From

this intermediate, NH₃ and Br⁻ ligands must interchange their coordination sites to produce an intermediate with the aryl and ammonia ligands in *cis* position, **III_C2**. Computational evaluation of the isomerization of these ligands on a Pd(II) square-planar complex is not an obvious task. Nevertheless, it has been experimentally shown that it is a rather easy process,^{61,62} thus, we can assume that the isomerization is feasible within this pathway.

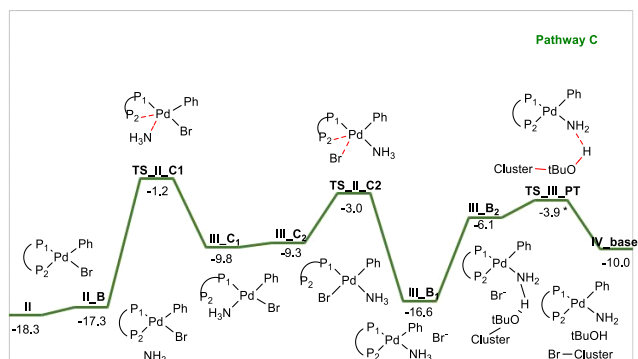


Figure 8: Gibbs energy profile involving phosphine dissociation of P₂ (Pathway C) in 1-4 dioxane (kcal mol⁻¹). * Value estimated in the absence of Br⁻ from the calculation.

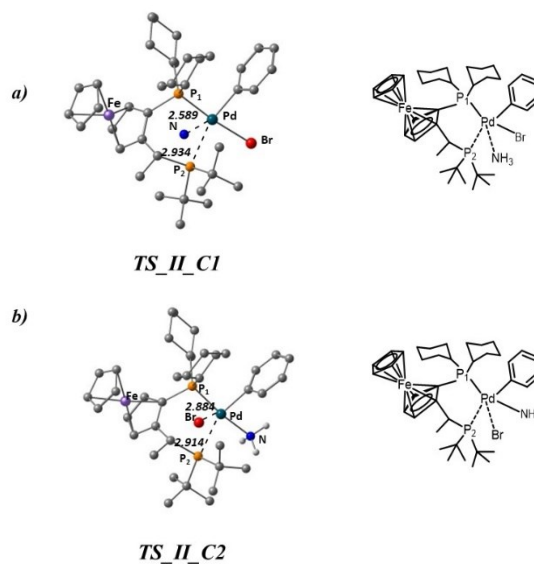


Figure 9: Optimized geometries for: (a) **TS_II_C1**, (b) **TS_II_C2**. Distances in Å.

In order to evaluate the relative energy of this new isomer **III_C2** a conformational analysis was also performed (see Supporting Information). The two most stable conformations are 2 and 3 (Table 1 and Figure 10). Conformation 3 is 2.7 kcal mol⁻¹ higher in energy than conformation 2. Nevertheless, conformation 3 has the appropriate geometrical disposition of the free phosphine arm to undertake the bromide by phosphine ligand substitution process. This means that although this conformation is higher in energy, it must be involved in this reaction path. Therefore, this conformation is the one included in the reaction profile (Figure 8).

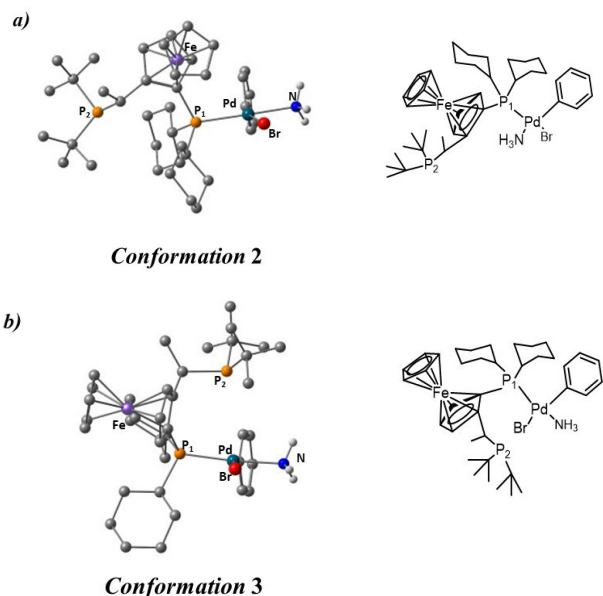


Figure 10. Optimized geometries for conformations of intermediate **III_C2**: (a) **2** and (b) **3**.

The isomerization evolves giving rise to intermediate **III_C2**, located at -9.3 kcal mol⁻¹ very close in energy to the preceding intermediate, **III_C1**. Next step is the association of the phosphine and replacement of the halide through transition state **TS_II_C2** (located at -3.0 kcal mol⁻¹; Figure 8). This step has a relative Gibbs energy barrier of 6.3 kcal mol⁻¹. The intermediate formed in this step is analogous to that obtained in pathway B, **III_B1**, with the phosphine dis-coordinated and the phenyl and NH₃ ligands in *cis* position. This point on the profile is analogous to that presented for pathway B, so structures were equally named.

- Pathway D

In this pathway the base plays a double role in the reaction, similarly to pathway A. The complete ligand substitution process occurs through three consecutive replacements: (i) the phosphine arm P₂ by the base, t-BuO⁻, (ii) bromide ligand by the incoming amine and finally (iii) the phosphine recovers the coordination site by replacing the base t-BuO⁻ along with the deprotonation of the coordinated amine.

As in the previous case, the replacement of the phosphine arm by the base generates an intermediate with a monodentate phosphine ligand that requires a conformational analysis to evaluate the most feasible intermediate. Like in the previous pathway (Scheme 2), two different isomers can be formed depending on which is the substituted arm of the phosphine. Releasing phosphine P₁ is more energetic than P₂, thus, the later was the only one considered. The results for the conformational analysis are gathered in Table 2 (see Supporting Information).

Table 2: Gibbs relative energies (kcal mol⁻¹) for conformers of intermediates **III_D1**, **III_D1'** and **III_D2**.

Conformations	$\Delta\Delta G_{\text{solv}}$	$\Delta\Delta G_{\text{solv}}$	$\Delta\Delta G_{\text{solv}}$
	III_D1	III_D1'	III_D2
Conf. 1	4.7	8.4	4.6
Conf. 2	5.2	16.6	6.1
Conf. 3	10.3	7.0	0.1
Conf. 4	0.0 ^a	8.3	7.9
Conf. 5	1.2	7.6	1.3
Conf. 6	0.5	16.8	-0.6 ^b
Conf. 7	2.6	22.8	2.0
Conf. 8	19.9	25.4	13.6
Conf. 9	19.1	17.5	14.1
Conf. 10	9.7	13.5	7.5

^a This conformation has a relative energy of -10.5 kcal mol⁻¹ within reaction profile in pathway D (Figure 11). ^b This conformation has a relative energy of 3.4 kcal mol⁻¹ within reaction profile in pathway D (Figure 11).

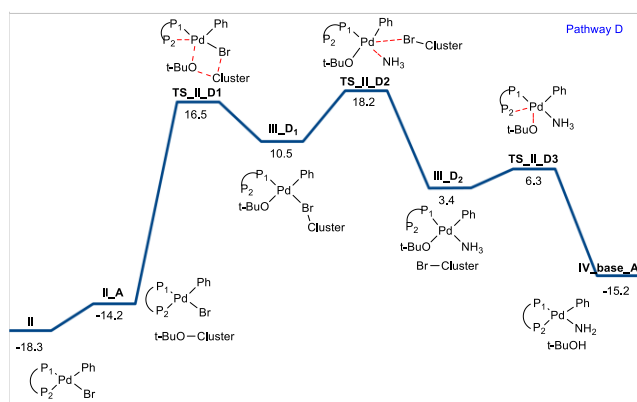


Figure 11: Gibbs energy profile involving phosphine dissociation of P₂ (Pathway D) in 1-4 dioxane (kcal mol⁻¹).

The Gibbs energy profile for this pathway is shown in Figure 11. The transition state for the first step, substitution of the phosphine P₂ by t-BuO⁻, (from (t-BuONa)₄) **TS_II_D1** (Figure 12), is located at 16.5 kcal mol⁻¹, with a relative Gibbs energy barrier of 34.8 kcal mol⁻¹. The intermediate formed, **III_D1**, has a relative energy of 10.5 kcal mol⁻¹ and corresponds to conformation **3** (Table 2). For the mechanistic analysis only the most stable conformation was considered (it does not modify the conclusions of the work since this pathway is discarded). Next step corresponds to the substitution of the bromide by ammonia, with a Gibbs energy for **TS_II_D2** of 18.2 kcal mol⁻¹. A conformational analysis was also performed for this intermediate, **III_D2**, with the most stable conformation located at 3.4 kcal mol⁻¹ (see Supporting Information). The last step corresponds to the replacement of the t-BuO⁻ by the phosphine arm, concomitantly to the proton transfer from the coordinated NH₃ ligand to the releasing base. This step goes through **TS_II_D3** with a relative Gibbs energy barrier of 2.9 kcal mol⁻¹ (Figure 12). The intermediate formed, **IV_base_A** (-15.2 kcal mol⁻¹), recovers the coordination of the biphosphine. Such an

intermediate is common for all analysed pathways. This is the highest energy pathway among all considered ones.

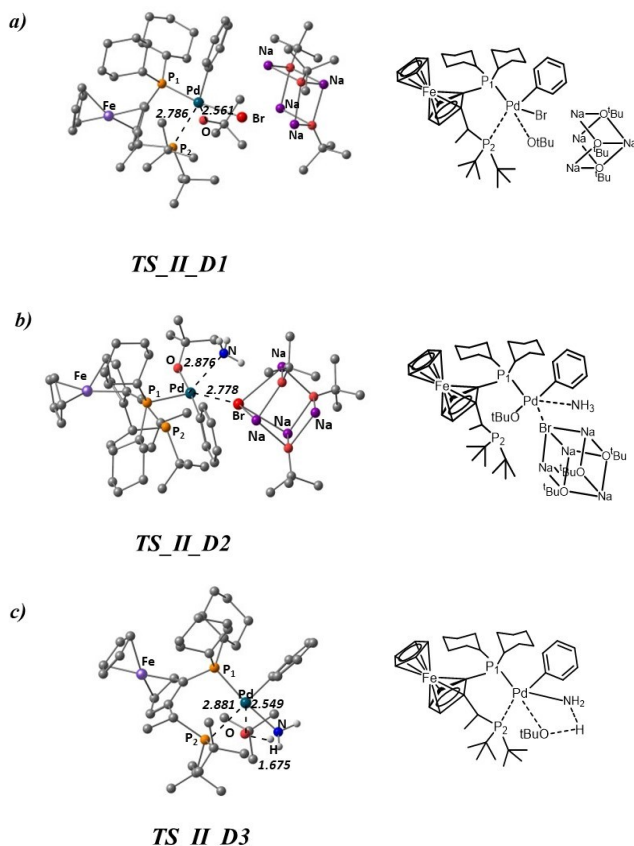


Figure 12: Optimized geometries for: (a) **TS_II_D1**, (b) **TS_II_D2** and (c) **TS_II_D3**. Distances in Å.

Reductive Elimination

The last step of the whole mechanism is the reductive elimination. It takes place from **IV** intermediate having NH_2^- and Ph ligands in *cis* position. It is located at $-12.1 \text{ kcal mol}^{-1}$; calculation performed without additional species in the model (Figure 13). As well as the oxidative addition, the reductive elimination is common for the four evaluated pathways (A, B, C and D). The Gibbs energy barrier for reductive elimination, through the transition state **TS_IV**, is $17.6 \text{ kcal mol}^{-1}$. The reductive elimination takes place through a concerted step. The formed intermediate **V** is located at $-34.6 \text{ kcal mol}^{-1}$. This intermediate contains the final product of the catalytic cycle for the Buchwald-Hartwig amination coordinated to the Pd center. Replacement of the product by the arylbromide reactant closes the catalytic cycle.

For the sake of completeness, the reductive elimination was also calculated for the other possible isomer where the Ph and NH_2^- ligands interchange their positions, intermediate **IV_op**. This intermediate is $3.4 \text{ kcal mol}^{-1}$ higher in energy than intermediate **IV**. The relative Gibbs energy barrier for this step, **TS_IV_op**, is also higher than that for

TS_IV by $3.1 \text{ kcal mol}^{-1}$. Both computed paths give rise to the formation of the same intermediate **V**.

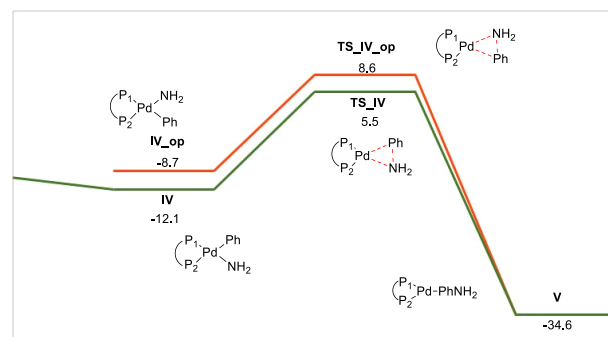


Figure 13: Energy Gibbs profile for the oxidative addition in 1-4 dioxane (kcal mol^{-1}).

Reaction Mechanism Proposed

In the previous section several pathways for the Pd-Josiphos catalyzed Buchwald-Hartwig amination of arylbromide using ammonia were evaluated. In this section we discuss these results.

The first and last steps, oxidative addition and reductive elimination, are common to any coupling reaction.^{5,63} Both steps are concerted. Since Josiphos is an asymmetric phosphine the oxidative addition may give rise to two different isomers, however, one of them, intermediate **II** is clearly kinetically and thermodynamically favoured. The oxidative addition has a rather low energy barrier as expected for a strong electron-donating and steric bulky ligand as Josiphos. The reductive elimination step is rate determining, in agreement with other computational studies^{37,39,39,40} and experiment.^{17,64}

For the ligand substitution process four different alternatives were considered, pathways A, B, C and D. The two first pathways proceed without dissociation of the phosphine, whereas the last two involve the dissociation of one of the phosphine arms of the bidentated ligand. The relative energy barriers for the step after the oxidative addition are 28.5 , 20.8 , 17.1 and $34.8 \text{ kcal mol}^{-1}$ for pathways A, B, C and D, respectively. Pathways B and C are the most feasible ones, with the later $3.7 \text{ kcal mol}^{-1}$ lower in energy than the former. Both pathways are analogous, in the sense that the amine replaces the bromide ligand, thus *t*-BuO⁻ only acts as a base. The difference between B and C comes from the fact that in C the phosphine dissociates one of the arms thus offering a new coordination site. In fact, the relative Gibbs energy barrier for any of these two paths is lower than that for reductive elimination. Therefore, according to these results both pathways can be operative during the process, though pathway C is the most favoured one.

A general scheme for the catalytic cycle is shown in Figure 14. It can be described by (i) oxidative addition, (ii) replacement of a phosphine arm by the ammonia ligand, (iii) isomerization of ligands NH_3 and Br^- respect to the aryl

group and replacement of the halide by the P₂ phosphine, (iv) deprotonation of coordinated amine by the base (t-BuO⁻), and (v) reductive elimination. The direct replacement of Br⁻ by NH₃ without releasing any of the chelate phosphine arms is also accessible (Figure 14 dashed arrow).

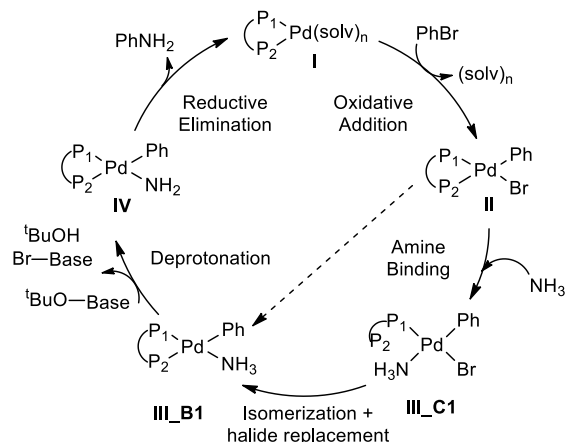


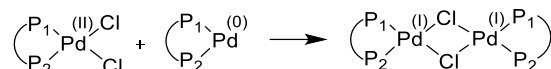
Figure 14: Catalytic cycle proposed for the Buchwald-Hartwig amination using a chelated Pd-complex and ammonia; (P₁-P₂ = Josiphos).

The mechanistic proposal for a Pd-catalyst with monophosphine ligand shows that for the ligand substitution process (see Figure 2), the catalyst substitutes the bromide ligand by the coordination of the amine along with the subsequent deprotonation.³⁷ In the case of the Pd-catalyst with the Josiphos chelate ligand, the mechanistic proposal introduces some differences. Although the analogous mechanism is feasible, in the preferred pathway the amine replaces a phosphine arm instead of the bromide. Then, after an isomerization the phosphine arm replaces the bromide to generate an intermediate ready for the reductive elimination.

For the ligand substitution process one can observe that replacing Br⁻ by NH₃ is more feasible than its replacement by t-BuO⁻. Moreover, the substitution of Br⁻ by NH₃ is also more favorable than the replacement of t-BuO⁻ by NH₃ (as found for intermediate III_D1 in pathway D). These factors together are behind the fact that the base, t-BuO⁻, is acting only as a base, and not as a ligand. These results are in line with previous suggestions that one of the arms of the BINAP phosphine is released during the reaction;³⁹ the authors were examining the relative energy of the feasible intermediates involved in the reaction without calculating the barriers; in those terms such proposal could be feasible although they did not exclude other possible pathways. Indeed, the present calculations including the energy barriers for all the ligand substitution steps shows that the phosphine does not remain coordinated along the mechanism. These results are somehow related to the conclusions reported by Baik³³ and Ma⁴¹ where they found for the case of the Buchwald phosphine, such ligand also generates a coordination site along the reaction pathway to be occupied by the amine. Moreover, in agreement with these

works, the reductive elimination has the highest Gibbs energy barrier.

For the sake of completeness, we also evaluated the possibility for the comproportionation between the active catalyst Pd⁰, and the precatalyst Pd^{II}Cl₂ intermediates to form the dimeric Pd(I) complex (Scheme 3). The presence of highly reactive Pd⁰ active species may promote the formation of other bimetallic species that can favor the process, or be detrimental, depending on the conditions.^{65,66,67,68} This reaction competes with the first step of the catalytic cycle, the oxidative addition step. For the formation of the dimeric complex we assumed that both Pd centers have a coordinated Josiphos chelated ligand.



Scheme 3: General scheme for Pd(0) + Pd(II) comproportionation.

The dimer formation has a ΔG of 13.0 kcal mol⁻¹, which indicates that the dimer is less stable than the separated reactants. The analysis of the structure shows that the complex has not the structural characteristics expected for a Pd(I)-Pd(I) dimer. The distance between both Pd atoms is 4.089 Å, much longer than the expected distance around 3 Å. Moreover, the geometry around one of the Pd centers is square planar whereas the other is tetrahedral. This geometrical arrangement around the metallic centers indicate that the bidentate complex corresponds to a Pd(II)-Pd(0) dimer. Several attempts to obtain the Pd(I)-Pd(I) dimer were performed, but when releasing all the fixed parameters the geometry converged to the one shown in Figure 15. Similar behaviour was found for the dimer with bromide as bridging ligands (see Figure S7). Therefore, the formation of Pd(I)-Pd(I) dimeric species can be discarded when chelating Josiphos phosphine is used as ligand.

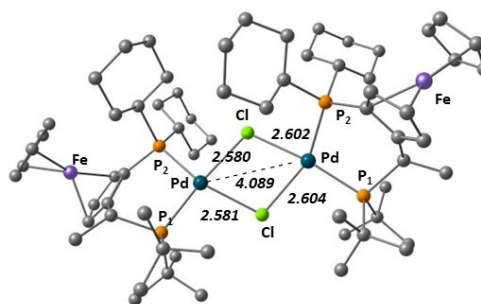


Figure 15: Optimized geometry for the Pd-Josiphos dimer. Distances in Å.

CONCLUSIONS

The C-N coupling between arylbromide and ammonia catalysed by Pd-Josiphos chelate complex is analyzed by means of DFT calculations. A general scheme for the catalytic cycle can be described as follows (Figure 14): (i) oxidative addition, (ii) replacement of a phosphine arm by the ammonia ligand, (iii) *cis-trans* isomerization of the ligands NH₃ and Br⁻ respect to the aryl group along with

replacement of the halide ligand by the phosphine arm, (iv) deprotonation of coordinated amine by the base ($t\text{-BuO}^-$), and (v) reductive elimination. The direct replacement of Br^- by NH_3 is slightly higher in energy but accessible.

The oxidative addition and reductive elimination steps are concerted.^{37,39} The oxidative addition shows a rather low energy barrier as expected for a bulky and electron-donating ligand as Josiphos. The reductive elimination step, however, shows the highest relative energy barrier for the process. These conclusions are in agreement with other experimental^{17,64} and computational studies.^{37,39} The possibility for the comproportionation between $\text{Pd}(\text{o})$ and $\text{Pd}(\text{II})$ species was evaluated obtaining that it is unfeasible for the Pd -Josiphos chelating system.

For the ligand substitution process four different pathways, A, B, C and D were evaluated: C and D involve dissociation of a phosphine arm, whereas for A and B the Josiphos remains fully coordinated to Pd center. The two feasible pathways B and C, both entail the replacement of the halide by the amine. The most favourable pathway, C, involves the dissociation of a phosphine arm along the process. A conformational analysis of the intermediate with open chelate is required to properly evaluate this path.

Regarding substitution patterns, replacement of Br^- by NH_3 at the coordination sphere of $\text{Pd}(\text{Josiphos})$ is more feasible than its replacement by $t\text{-BuO}^-$. The substitution of Br^- by NH_3 is also more favourable than the replacement of $t\text{-BuO}^-$ by NH_3 . Thus, the $t\text{-BuO}^-$ does not act as a ligand in this process, acting only as a base. The ligand substitution process follows a similar trend for mono- or bidentated phosphine catalysts.

Overall, we analyzed the reaction mechanism for the Pd -Josiphos catalyzed C-N coupling of arylbromide with NH_3 identifying the role of the chelating phosphine and the base providing useful information for rational design of new chelating ligands.

EXPERIMENTAL SECTION

Computational Data. Calculations were performed using the Mo6 functional⁶⁹ with an ultrafine grid, as implemented in Gaussian 09.⁷⁰ The Pd atom was described using the scalar relativistic Stuttgart–Dresden SDD pseudopotential and its associated double- ζ basis set, complemented with a set of off functions.⁷¹ The $6\text{-}311\text{G}(\text{d},\text{p})$ basis set was used for the rest of atoms. The structures of the reactants, products, intermediates and transition states were optimized in 1,4-dioxane solvent ($\epsilon=2.25$), described by the SMD polarizable continuum model.⁷² The nature of the stationary points was confirmed by frequency analysis. Connections between the transition states and the minima were checked by following the IRC and subsequent geometry optimization until the corresponding minima. Cartesian coordinates for the supporting information were generated by EsiGen software.⁷³

Gibbs energies in 1,4-dioxane were calculated at 298 K. A correction of $1.9 \text{ kcal mol}^{-1}$ was applied to all Gibbs energies calculated to change the standard state from the gas phase (1 bar) to solution (1 M).⁷⁴ Thermal contributions to the Gibbs energies were corrected by employing the approximation described by Grimme⁷⁵ where entropic terms for frequencies below a cut-off (100 cm^{-1}), were calculated using the free-rotor approximation. The GoodVibes program developed by Paton and Funes-Ardoiz was employed to introduce these corrections.⁷⁶

The system selected for the theoretical study includes the bidentate (Josiphos) coordinated to Pd catalyst, PhBr and NH_3 as substrates and $(t\text{-BuONa})_4$ as base; the model for the base was a tetrameric form considering the non-polar environment of the reaction, as illustrated in the Figure 16.^{33, 77,78} These species were selected according to experiments made by Hartwig and co-workers.^{17,18,64} We took the X-ray crystallographic structure of Josiphos ligand coordinated to Pd ⁶⁴ as starting point for optimizing the geometries. Josiphos is not symmetric with P_1 and P_2 bearing cyclohexyls and isobutyls, respectively (Figure 16).

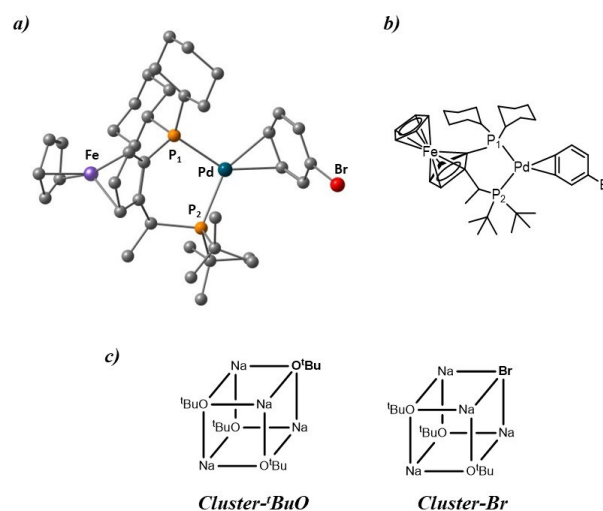


Figure 16. (a) Optimized structure for $\text{Pd}(\text{Josiphos})(\text{PhBr})$, intermediate I. (b) Scheme of the intermediate I. (c) Schematic illustration of base as tetrameric form $(t\text{-BuONa})_4$, cluster- $t\text{-BuO}$, and $[(t\text{-BuO})_3\text{BrNa}_4]$, cluster- Br .

Pathways considering dissociation of one of the phosphine arms were also considered. To obtain a proper conformation of the catalyst we performed a conformational study on such intermediates. For such analysis classical MD simulations were performed at constant temperature using Amber 16.⁷⁹ The temperature was set at 1000 K to ensure a wide exploration of the conformational space. The scheme developed by Merz⁸⁰ to obtain force field parameters compatible with the Amber force field⁷⁹ based on the Seminario method⁸¹ was employed. Calculations were performed under solvent-free conditions. A 1 fs time step was used to integrate the equations of motion, for a total simulation time of 10 ns. Coordinates were saved every 1000 steps, for a total of 10000 structures. The k-means

clustering method⁸² was applied to those structures obtaining ten different clusters. The most representative structure for each of the clusters was subsequently optimized at the same DFT level to check the feasibility of these conformers and their relative Gibbs energy.

ASSOCIATED CONTENT

Supporting Information. Figures of relevant structures; information about a transition state search; cartesian coordinates. This material is available free of charge via the Internet at <http://pubs.acs.org>.”

AUTHOR INFORMATION

Corresponding Author

Agustí Lledós – Departament de Química, Universitat Autònoma de Barcelona and Centro de Innovació en Química Avanzada (ORFEO-CINQA), 08193 Cerdanyola del Vallès, Catalonia, Spain;

orcid.org/0000-0001-7909-422X;

Email: agusti@klingon.uab.es

Gregori Ujaque – Departament de Química, Universitat Autònoma de Barcelona and Centro de Innovació en Química Avanzada (ORFEO-CINQA), 08193 Cerdanyola del Vallès, Catalonia, Spain;

orcid.org/0000-0001-5896-9998;

Email: gregori.ujaque@uab.cat

ACKNOWLEDGMENT

Support from the Spanish MINECO is acknowledged (CTQ2017-87889-P, Red ORFEO-CINQA (CTQ2016-81797-REDC) FPU Grant (to P. G.-O., BES-2015-07419)).

REFERENCES

- (1) Hartwig, J. F. Carbon–Heteroatom Bond Formation Catalysed by Organometallic Complexes. *Nature* **2008**, *455*, 314–322.
- (2) Surry, D. S.; Buchwald, S. L. Dialkylbiaryl Phosphines in Pd-Catalyzed Amination: A User’s Guide. *Chem. Sci.* **2011**, *2*, 27–50.
- (3) Hartwig, J. F. Transition Metal Catalyzed Synthesis of Arylamines and Aryl Ethers from Aryl Halides and Triflates: Scope and Mechanism. *Angew. Chem., Int. Ed.* **1998**, *37*, 2046–2067.
- (4) Buchwald, S. L.; Hartwig, J. F. In Praise of Basic Research as a Vehicle to Practical Applications: Palladium-Catalyzed Coupling to Form Carbon-Nitrogen Bonds. *Isr. J. Chem.* **2020**, *60*, 177–179.
- (5) Buchwald, S. L. Cross Coupling. *Acc. Chem. Res.* **2008**, *41*, 1439.
- (6) Hartwig, J. F. *Organotransition Metal Chemistry: From Bonding to Catalysis*; University Science Books, 2010.
- (7) Bariwal, J.; Van Der Eycken, E. C-N Bond Forming Cross-Coupling Reactions: An Overview. *Chem. Soc. Rev.* **2013**, *42*, 9283–9303.
- (8) Freire De Queiroz, J.; Walkimar, J.; Carneiro, M.; Sabino, A. A.; Sparrapan, R.; Eberlin, M. N.; Esteves, P. M. Electrophilic Aromatic Nitration: Understanding Its Mechanism and Substituent Effects. *J. Org. Chem.* **2006**, *71*, 6192–6203.
- (9) Nayal, O. S.; Bhatt, V.; Sharma, S.; Kumar, N. Chemoselective Reductive Amination of Carbonyl Compounds for the Synthesis of Tertiary Amines Using SnCl₂·2H₂O/PMHS/MeOH. *J. Org. Chem.* **2015**, *80*, 5912–5918.
- (10) Shin, K.; Kim, H.; Chang, S. Transition-Metal-Catalyzed C-N Bond Forming Reactions Using Organic Azides as the Nitrogen Source: A Journey for the Mild and Versatile C-H Amination. *Acc. Chem. Res.* **2015**, *48*, 1040–1052.
- (11) Ruiz-Castillo, P.; Buchwald, S. L. Applications of Palladium-Catalyzed C–N Cross-Coupling Reactions. *Chem. Rev.* **2016**, *116*, 12564–12649.
- (12) Van der Vlugt, J. I. Advances in Selective Activation and Application of Ammonia in Homogeneous Catalysis. *Chem. Soc. Rev.* **2010**, *39*, 2302–2322.
- (13) Klinkenberg, J. L.; Hartwig, J. F. Catalytic Organometallic Reactions of Ammonia. *Angew. Chem., Int. Ed.* **2011**, *50*, 86–95.
- (14) Aubin, Y.; Fischmeister, C.; Thomas, C. M.; Renaud, J. L. Direct Amination of Aryl Halides with Ammonia. *Chem. Soc. Rev.* **2010**, *39*, 4130–4145.
- (15) Schranck, J.; Tlili, A. Transition-Metal-Catalyzed Monoarylation of Ammonia. *ACS Catal.* **2018**, *8*, 405–418.
- (16) Streiff, S.; Jérôme, F. Hydroamination of Non-Activated Alkenes with Ammonia: A Holy Grail in Catalysis. *Chem. Soc. Rev.* **2021**.
- (17) Vo, G. D.; Hartwig, J. F. Palladium-Catalyzed Coupling of Ammonia with Aryl Chlorides, Bromides, Iodides, and Sulfonates: A General Method for the Preparation of Primary Arylamines. *J. Am. Chem. Soc.* **2009**, *131*, 11049–11061.
- (18) Shen, Q.; Hartwig, J. F. Palladium-Catalyzed Coupling of Ammonia and Lithium Amide with Aryl Halides. *J. Am. Chem. Soc.* **2006**, *128*, 10028–10029.
- (19) Surry, D. S.; Buchwald, S. L. Selective Palladium-Catalyzed Arylation of Ammonia: Synthesis of Anilines as Well as Symmetrical and Unsymmetrical Di- and Triarylamines. *J. Am. Chem. Soc.* **2007**, *129*, 10354–10355.
- (20) Cheung, C. W.; Surry, D. S.; Buchwald, S. L. Mild and Highly Selective Palladium-Catalyzed Monoarylation of Ammonia Enabled by the Use of Bulky Biarylphosphine Ligands and Palladacycle Precatalysts. *Org. Lett.* **2013**, *15*, 3734–3737.
- (21) Gross, T.; Seayad, A. M.; Ahmad, M.; Beller, M. Synthesis of Primary Amines: First Homogeneously Catalyzed Reductive Amination with Ammonia. *Org. Lett.* **2002**, *4*, 2055–2058.
- (22) Zimmermann, B.; Herwig, J.; Beller, M. The First Efficient Hydroaminomethylation with Ammonia: With Dual Metal Catalysts and Two-Phase Catalysis to Primary Amines. *Angew. Chem., Int. Ed.* **1999**, *38*, 2372–2375.
- (23) Nagano, T.; Kobayashi, S. Palladium-Catalyzed Allylic Amination Using Aqueous Ammonia for the Synthesis of Primary Amines. *J. Am. Chem. Soc.* **2009**, *131*, 4200–4201.
- (24) Lavallo, V.; Frey, G. D.; Donnadiou, B.; Soleilhavoup, M.; Bertrand, G. Homogeneous Catalytic Hydroamination

- of Alkynes and Allenes with Ammonia. *Angew. Chem., Int. Ed.* **2008**, *47*, 5224–5228.
- (25) Pouy, M. J.; Stanley, L. M.; Hartwig, J. F. Enantioselective, Iridium-Catalyzed Monoallylation of Ammonia. *J. Am. Chem. Soc.* **2009**, *131*, 11312–11313.
- (26) Xia, N.; Taillefer, M. A Very Simple Copper-Catalyzed Synthesis of Anilines by Employing Aqueous Ammonia. *Angew. Chem., Int. Ed.* **2009**, *48*, 337–339.
- (27) Gunanathan, C.; Milstein, D. Selective Synthesis of Primary Amines Directly from Alcohols and Ammonia. *Angew. Chem., Int. Ed.* **2008**, *47*, 8661–8664.
- (28) Lundgren, R. J.; Peters, B. D.; Alsabeh, P. G.; Stradiotto, M. A P,N-Ligand for Palladium-Catalyzed Ammonia Arylation: Coupling of Deactivated Aryl Chlorides, Chemoselective Arylations, and Room Temperature Reactions. *Angew. Chem., Int. Ed.* **2010**, *49*, 4071–4074.
- (29) Kovács, G.; Lledós, A.; Ujaque, G. Hydroamination of Alkynes with Ammonia: Unforeseen Role of the Gold(I) Catalyst. *Angew. Chem., Int. Ed.* **2011**, *50*, 11147–11151.
- (30) Stirling, A.; Nair, N. N.; Lledós, A.; Ujaque, G. Challenges in Modelling Homogeneous Catalysis: New Answers from Ab Initio Molecular Dynamics to the Controversy over the Wacker Process. *Chem. Soc. Rev.* **2014**, *43*, 4940–4952.
- (31) Couce-Rios, A.; Kovács, G.; Ujaque, G.; Lledós, A. Hydroamination of C-C Multiple Bonds with Hydrazine Catalyzed by N-Heterocyclic Carbene-Gold(I) Complexes: Substrate and Ligand Effects. *ACS Catal.* **2015**, *5*, 815–829.
- (32) Muñoz-López, S.; Couce-Rios, A.; Sciortino, G.; Lledós, A.; Ujaque, G. Mechanistic Insights on the Hydration of Terminal and Internal Allenes Catalyzed by [(NHC)Au]⁺. *Organometallics* **2018**, *37*, 3543–3551.
- (33) Kim, S. T.; Kim, S.; Baik, M. H. How Bulky Ligands Control the Chemoselectivity of Pd-Catalyzed: N-Arylation of Ammonia. *Chem. Sci.* **2020**, *11*, 1017–1025.
- (34) Harvey, J. N.; Himo, F.; Maseras, F.; Perrin, L. Scope and Challenge of Computational Methods for Studying Mechanism and Reactivity in Homogeneous Catalysis. *ACS Catal.* **2019**, *9*, 6803–6813.
- (35) Eisenstein, O.; Ujaque, G.; Lledós, A. What Makes a Good (Computed) Energy Profile?. In: Lledós A., Ujaque, G. (eds) *New Directions in the Modeling of Organometallic Reactions. Top. in Organomet. Chem.* **2020**, *67*, 1-38.
- (36) Cundari, T. R.; Deng, J. Density Functional Theory Study of Palladium-Catalyzed Aryl-Nitrogen and Aryl-Oxygen Bond Formation. *J. Phys. Org. Chem.* **2005**, *18*, 417–425.
- (37) McMullin, C. L.; R., B.; Besora, M.; Orpen, A. G.; Harvey, J. N.; Fey, N. Computational Study of PtBu₃ as Ligand in the Palladium-Catalyzed Amination of Phenylbromide with Morpholine. *J. Mol. Catal. A Chem.* **2010**, *324*, 48–55.
- (38) Hoi, K. H.; Çalimsiz, S.; Froese, R. D. J.; Hopkinson, A. C.; Organ, M. G. Amination with Pd–NHC Complexes: Rate and Computational Studies on the Effects of the Oxidative Addition Partner. *Chem. – A Eur. J.* **2011**, *17*, 3086–3090.
- (39) Sunesson, Y.; Lime, E.; Lill, S. O. N.; Meadows, R. E.; Norrby, P.-O. Role of the Base in Buchwald – Hartwig Amination. *J. Org. Chem.* **2014**, *79*, 11961–11969.
- (40) Kim, S. T.; Pudasaini, B.; Baik, M. H. Mechanism of Palladium-Catalyzed C-N Coupling with 1,8-Diazabicyclo[5.4.0]Undec-7-Ene (DBU) as a Base. *ACS Catal.* **2019**, *9*, 6851–6856.
- (41) Tian, J.; Wang, G.; Qi, Z.-H.; Ma, J. Ligand Effects of BrettPhos and RuPhos on Rate-Limiting Steps in Buchwald–Hartwig Amination Reaction Due to the Modulation of Steric Hindrance and Electronic Structure. **2020**.
- (42) Scharf, L. T.; Rodstein, I.; Schmidt, M.; Scherpf, T.; Gessner, V. H. Unraveling the High Activity of Ylide-Functionalized Phosphines in Palladium-Catalyzed Amination Reactions: A Comparative Study with CyJohnPhos and PtBu₃. *ACS Catal.* **2020**, *10*, 999–1009.
- (43) Yong, F. F.; Mak, A. M.; Wu, W.; Sullivan, M. B.; Robins, E. G.; Johannes, C. W.; Jong, H.; Lim, Y. H. Empirical and Computational Insights into N-Arylation Reactions Catalyzed by Palladium Meta-Tertiaryphosphine Catalyst. *ChemPlusChem.* **2017**, *82*, 750–757.
- (44) Lombardi, C.; Rucker, R. P.; Froese, R. D. J.; Sharif, S.; Champagne, P. A.; Organ, M. G. Rate and Computational Studies for Pd-NHC-Catalyzed Amination with Primary Alkylamines and Secondary Anilines: Rationalizing Selectivity for Monoarylation versus Diarylation with NHC Ligands. *Chem. – A Eur. J.* **2019**, *25*, 14223–14229.
- (45) Shekhar, S.; Hartwig, J. F. Effects of Bases and Halides on the Amination of Chloroarenes Catalyzed by Pd(PtBu₃)₂. *Organometallics* **2007**, *26*, 340–351.
- (46) Tardiff, B. J.; McDonald, R.; Ferguson, M. J.; Stradiotto, M. Rational and Predictable Chemoselective Synthesis of Oligoamines via Buchwald–Hartwig Amination of (Hetero)Aryl Chlorides Employing Mor-Dalphos. *J. Org. Chem.* **2012**, *77*, 1056–1071.
- (47) Ohmiya, H.; Moriya, T.; Sawamura, M. Cu(I)-Catalyzed Intramolecular Hydroamination of Unactivated Alkenes Bearing a Primary or Secondary Amino Group in Alcoholic Solvents. *Org. Lett.* **2009**, *11*, 2145–2147.
- (48) Wolfe, J. P.; Wagaw, S.; Marcoux, J. F.; Buchwald, S. L. Rational Development of Practical Catalysts for Aromatic Carbon-Nitrogen Bond Formation. *Acc. Chem. Res.* **1998**, *31*, 805–818.
- (49) Shekhar, S.; Ryberg, P.; Hartwig, J. F.; Mathew, J. S.; Blackmond, D. G.; Strieter, E. R.; Buchwald, S. L. Reevaluation of the Mechanism of the Amination of Aryl Halides Catalyzed by BINAP-Ligated Palladium Complexes. *J. Am. Chem. Soc.* **2006**, *128*, 3584–3591.
- (50) Thomas, G. T.; Janusson, E.; Zijlstra, H. S.; McIndoe, J. S. Step-by-Step Real Time Monitoring of a Catalytic Amination Reaction. *Chem. Commun.* **2019**, *55*, 11727–11730.
- (51) Dennis, J. M.; White, N. A.; Liu, R. Y.; Buchwald, S. L. Pd-Catalyzed C-N Coupling Reactions Facilitated by Organic Bases: Mechanistic Investigation Leads to Enhanced Reactivity in the Arylation of Weakly Binding Amines. *ACS Catal.* **2019**, *9*, 3822–3830.
- (52) Besora, M.; Maseras, F. The Diverse Mechanisms for the Oxidative Addition of C-Br Bonds to Pd(PR₃) and Pd(PR₃)₂ Complexes. *Dalt. Trans.* **2019**, *48*, 16242–16248.
- (53) Ahlquist, M.; Norrby, P. O. Oxidative Addition of Aryl

- Chlorides to Monoligated Palladium(0): A DFT-SCRF Study. *Organometallics* **2007**, *26*, 550–553.
- (54) Barder, T. E.; Biscoe, M. R.; Buchwald, S. L. Structural Insights into Active Catalyst Structures and Oxidative Addition to (Biaryl)Phosphine - Palladium Complexes via Density Functional Theory and Experimental Studies. *Organometallics* **2007**, *26*, 2183–2192.
- (55) McMullin, C. L.; Fey, N.; Harvey, J. N. Computed Ligand Effects on the Oxidative Addition of Phenyl Halides to Phosphine Supported Palladium(0) Catalysts. *Dalt. Trans.* **2014**, *43*, 13545–13556.
- (56) Gourlaouen, C.; Ujaque, G.; Lledós, A.; Medio-Simon, M.; Asensio, G.; Maseras, F. Why Is the Suzuki-Miyaura Cross-Coupling of Sp³ Carbons in α -Bromo Sulfoxide Systems Fast and Stereoselective? A DFT Study on the Mechanism. *J. Org. Chem.* **2009**, *74*, 4049–4054.
- (57) McMullin, C. L.; Jover, J.; Harvey, J. N.; Fey, N. Accurate Modelling of Pd(0) + PhX Oxidative Addition Kinetics. *Dalt. Trans.* **2010**, *39*, 10833–10836.
- (58) The Transition State for the Proton Transfer Could Not Be Located When Br⁻ Was Present in the Calculation; It Was Characterized by Removing Br⁻ from the Model; See Supporting Information.
- (59) Besora, M.; Braga, A. C.; Ujaque, G.; Maseras, F.; Lledós, A. The Importance of Conformational Search: A Test Case on the Catalytic Cycle of the Suzuki–Miyaura Cross-Coupling. *Theor. Chem. Acc.* **2018**, *128*, 636–646.
- (60) Munkerup, K.; Thulin, M.; Tan, D.; Lim, X.; Lee, R.; Huang, K. W. Importance of Thorough Conformational Analysis in Modelling Transition Metal-Mediated Reactions: Case Studies on Pincer Complexes Containing Phosphine Groups. *J. Saudi Chem. Soc.* **2019**, *23*, 1206–1218.
- (61) Pérez-Temprano, M. H.; Gallego, A. M.; Casares, J. A.; Espinet, P. Stille Coupling of Alkynyl Stannane and Aryl Iodide, a Many-Pathways Reaction: The Importance of Isomerization. *Organometallics* **2011**, *30*, 611–617.
- (62) García-Melchor, M.; Fuentes, B.; Lledós, A.; Casares, J. A.; Ujaque, G.; Espinet, P. Cationic Intermediates in the Pd-Catalyzed Negishi Coupling. Kinetic and Density Functional Theory Study of Alternative Transmetalation Pathways in the Me-Me Coupling of ZnMe₂ and Trans - [PdMeCl(PMePh₂)₂]. *J. Am. Chem. Soc.* **2011**, *133*, 13519–13526.
- (63) García-Melchor, M.; Braga, A. A. C.; Lledós, A.; Ujaque, G.; Maseras, F. Computational Perspective on Pd-Catalyzed C-C Cross-Coupling Reaction Mechanisms. *Acc. Chem. Res.* **2013**, *46*, 2626–2634.
- (64) Klinkenberg, J. L.; Hartwig, J. F. Slow Reductive Elimination from Arylpalladium Parent Amido Complexes. *J. Am. Chem. Soc.* **2010**, *132*, 11830–11833.
- (65) Balcells, D.; Nova, A. Designing Pd and Ni Catalysts for Cross-Coupling Reactions by Minimizing Off-Cycle Species. *ACS Catal.* **2018**, *8*, 3499–3515.
- (66) Bonney, K. J.; Schoenebeck, F. Experiment and Computation: A Combined Approach to Study the Reactivity of Palladium Complexes in Oxidation States 0 to IV. *Chem. Soc. Rev.* **2014**, *43*, 6609–6638.
- (67) Hruszkewycz, D. P.; Guard, L. M.; Balcells, D.; Feldman, N.; Hazari, N.; Tilset, M. Effect of 2-Substituents on Allyl-Supported Precatalysts for the Suzuki-Miyaura Reaction: Relating Catalytic Efficiency to the Stability of Palladium(I) Bridging Allyl Dimers. *Organometallics* **2015**, *34*, 381–394.
- (68) Johansson Seechurn, C. C. C.; Sperger, T.; Scrase, T. G.; Schoenebeck, F.; Colacot, T. J. Understanding the Unusual Reduction Mechanism of Pd(II) to Pd(I): Uncovering Hidden Species and Implications in Catalytic Cross-Coupling Reactions. *J. Am. Chem. Soc.* **2017**, *139*, 5194–5200.
- (69) Zhao, Y.; Truhlar, D. G. The M06 Suite of Density Functionals for Main Group Thermochemistry, Thermochemical Kinetics, Noncovalent Interactions, Excited States, and Transition Elements: Two New Functionals and Systematic Testing of Four M06-Class Functionals and 12 Other Functionals. *Theor. Chem. Acc.* **2008**, *120*, 215–241.
- (70) Frisch, M. J. et al. Gaussian09 Revision D.01, Gaussian Inc. Wallingford CT, 2010.
- (71) Ehlers, A. W.; Böhme, M.; Dapprich, S.; Gobbi, A.; Höllwarth, A.; Jonas, V.; Köhler, K. F.; Stegmann, R.; Veldkamp, A.; Frenking, G. A Set of F-Polarization Functions for Pseudo-Potential Basis Sets of the Transition Metals Sc-Cu, Y-Ag and La-Au. *Chem. Phys. Lett.* **1993**, *208*, 111–114.
- (72) Marenich, A. V.; Cramer, C. J.; Truhlar, D. G. Universal Solvation Model Based on Solute Electron Density and on a Continuum Model of the Solvent Defined by the Bulk Dielectric Constant and Atomic Surface Tensions. *J. Phys. Chem. B* **2009**, *113*, 6378–6396.
- (73) Rodríguez-Guerra Pedregal, J.; Gómez-Orellana, P.; Maréchal, J. D. ESIgen: Electronic Supporting Information Generator for Computational Chemistry Publications. *J. Chem. Inf. Model.* **2018**, *58*, 561–564.
- (74) Jensen, J. H. Predicting Accurate Absolute Binding Energies in Aqueous Solution: Thermodynamic Considerations for Electronic Structure Methods. *Phys. Chem. Chem. Phys.* **2015**, *17*, 12441–12451.
- (75) Grimme, S. Supramolecular Binding Thermodynamics by Dispersion-Corrected Density Functional Theory. *Chem. - A Eur. J.* **2012**, *18*, 9955–9964.
- (76) Funes-Ardoiz, I.; Paton, R. S. GoodVibes: GoodVibes v1.0.1. August 24, 2016.
- (77) Seebach, D. Structure and Reactivity of Lithium Enolates. From Pinacolone to Selective C-Alkylations of Peptides. Difficulties and Opportunities Afforded by Complex Structures. *Angew. Chem., Int. Ed.* **1988**, *27*, 1624–1654.
- (78) Liu, W. B.; Schuman, D. P.; Yang, Y. F.; Toutov, A. A.; Liang, Y.; Klare, H. F. T.; Nesnas, N.; Oestreich, M.; Blackmond, D. G.; Virgil, S. C.; Banerjee, S.; Zare, R. N.; Grubbs, R. H.; Houk, K. N.; Stoltz, B. M. Potassium Tert-Butoxide-Catalyzed Dehydrogenative C-H Silylation of Heteroaromatics: A Combined Experimental and Computational Mechanistic Study. *J. Am. Chem. Soc.* **2017**, *139*, 6867–6879.
- (79) Case, D. A.; Betz, R. M.; Cerutti, D. S.; T.E., C. I.; Darden, T. A.; Duke, R. E.; Giese, T. J.; Gohlke, H.; Goetz, A. W.; Homeyer, N.; Izadi, S.; Janowski, P.; Kaus, J.; Kovalenko, A.; Lee, T. S.; LeGrand, S.; Li, P.; C.Lin; Luchko, T.; Luo, R.; Madej, B.; Mermelstein, D.; Merz, K. M.; Monard, G.; Nguyen, H. T.; Nguyen, H. T.; Omelyan, I.; Onufriev, A.; Roe, D. R.; Roitberg, A.

- Sagui, C.; Simmerling, C. L.; Botello-Smith, W. M.; Swails, J.; Walker, R. C.; Wang, J.; Wolf, R. M.; Wu, X.; Xiao, L.; Kollman, P. A. Amber 2016. *University of California, San Francisco*. 2016.
- (80) Li, P.; Merz, K. M. MCPB.Py: A Python Based Metal Center Parameter Builder. *J. Chem. Inf. Model.* **2016**, *56*, 599–604.
- (81) Seminario, J. M. Calculation of Intramolecular Force Fields from Second-derivative Tensors. *Int. J. Quantum Chem.* **1996**, *60*, 1271–1277.
- (82) Wagstaff, K.; Cardie, C.; Rogers, S.; Schrödl, S. Constrained K-Means Clustering with Background Knowledge. *Int. Conf. Mach. Learn. ICML* **2001**, 577–584.
-